Analytical and numerical investigation of strain-hardening viscoplastic thick-walled cylinders under internal pressure by using sequential limit analysis

S.-Y. Leu [*]

Department of Aviation Mechanical Engineering, China Institute of Technology, No. 200, Jhonghua Street, Hengshan Township, Hsinchu County 312, Taiwan, ROC

Abstract

Plastic limit load of strain-hardening viscoplastic thick-walled cylinders subjected to internal pressure is investigated numerically and analytically in the paper. The paper applies sequential limit analysis to deal with the quasi-static problem involving hardening material properties and weakening behavior corresponding to the strain-rate sensitivity and widening deformation. By sequential limit analysis, the paper treats the plasticity problems as a sequence of limit analysis problems stated in the upper bound formulation. Rigorous upper bounds are acquired iteratively through a computational optimization procedure with the internal pressure factor as the objective function. Especially, rigorous validation was conducted by numerical and analytical studies of thick-walled cylinders in terms of the plastic limit load as well as the onset of instability. It is found that the computed limit loads are rigorous upper bounds and agree very well with the analytical solutions.
© 2007 Elsevier B.V. All rights reserved.

Keywords: Sequential limit analysis; von Mises criterion; Nonlinear isotropic hardening; Viscoplasticity; Hölder inequality; Thick-walled cylinder

1. Introduction

Limit analysis features in capturing directly the important information for structural design or safety evaluation. Especially, it is considered to play the role of a snapshot look at the structural performance while providing the limit solution based on only simple input data (see, for example [16]). Thus, as well known, limit analysis is applied effectively to bound rigorously the asymptotic behavior of an elastic-plastic material by the lower bound or the upper bound theorem.

On the one hand, we can state theoretically the equality relation between the greatest lower bound and the least upper bound by duality (minimax) theorems as demonstrated by Yang [37,39,40,42], and Huh and Yang [16]

mainly based on the generalized Hölder inequality [41]. On the other hand, it is numerically possible to enhance the accuracy of limit analysis and broaden its applicability to more complex problems in engineering applications as presented by Anderheggen and Knöpfel [1], Bottero et al. [3], Capsoni and Corradi [5], Christiansen [7], Corradi et al. [10], Dang Hung [11], Hodge and Belytschko [15], Pastor et al. [29], Sloan [34], Yang [40], Zhang et al. [43] by the use of finite element methods [33] together with mathematical programming techniques [25].

Furthermore, the fact that sequential limit analysis is an accurate and efficient tool for the large deformation analysis has been illustrated extensively by Corradi et al. [8], Corradi and Panzeri [9], Huh and Lee [17], Huh et al. [18], Hwan [19], Kim and Huh [22], Leu [26,27], Leu and Chen [28] and Yang [42]. By sequential limit analysis, a sequence of limit analysis problems is conducted sequentially with updating local yield criteria in addition to the

* Fax: +886 3 5936297.
E-mail address: syleu@cc.chit.edu.tw

configuration of the deforming structures. In each step and therefore the whole deforming process, rigorous upper bound or lower bound solutions are supposedly acquired sequentially as to bound the real limit solutions. Especially, a combined smoothing and successive approximation (CSSA) algorithm presented by Yang [38] has been utilized successfully with satisfactory results at a modest cost in certain problems of limit analysis by Huh and Yang [16] and sequential limit analysis by Huh and Lee [17], Huh et al. [18], Hwan [19], Kim and Huh [22], Leu [26,27], Leu and Chen [28] and Yang [42]. Particularly, some quantitative comparisons with elasto-plastic analysis have been made recently by Huh and his coworker [22]. As demonstrated in simulating the crashworthiness of structural members by Kim and Huh [22], only a fraction of the cost of elasto-plastic analysis was spent by sequential limit analysis. However, the unconditional convergence and numerical accuracy of the CSSA algorithm were demonstrated mostly by practical applications. Novelly, its convergence analysis was recently performed and validation was also conducted rigorously while extending the CSSA algorithm further to sequential limit analysis of viscoplasticity problems by Leu [26], or involving materials with nonlinear isotropic hardening by Leu [27].

In the literature, flow problems involving viscoplastic materials has been widely investigated using finite element methods (see, for example, [2,4,24,26,35]). On the other hand, the constitutive laws of viscoplastic materials have been often utilized to problems of regularized limit analysis (see, for example, [20,21,36]). In regularized limit analysis, the creep-strain rate is expected to converge to plastic-strain rates, see Jiang [20]. Based on the concept of sequential limit analysis, Leu [26] treated viscoplastic flow problems as a sequence of limit analysis problems. In each step of a deformation sequence, the limit load was computed by using the CSSA algorithm. Especially, the extended CSSA algorithm was shown to be unconditionally convergent by utilizing the Hölder inequality.

Leu [27] presented sequential limit analysis of plane-strain problems of the von Mises model with nonlinear isotropic hardening by using the CSSA algorithm. Particularly, the CSSA algorithm was proved to be unconditionally convergent by utilizing the Cauchy–Schwarz inequality in the work of Leu [27]. On the other hand, Leu and Chen [28] further applied the CSSA algorithm for sequential limit analysis involving nonlinear isotropic hardening materials to seek plastic limit angular velocity of rotating hollow cylinders.

Based on the previously successful applications in viscoplasticity [26] and nonlinear isotropic hardening problems [27,28], the paper aims to extend further the above-mentioned CSSA algorithm to upper-bound limit analysis considering the combination effect of strain hardening and viscoplasticity. Especially, numerical convergence of the CSSA algorithm is to be shown by means of the Hölder inequality. Particularly, the applicability of the CSSA algorithm is to be validated by numerical and analytical studies

of thick-walled cylinders under internal pressure involving materials made of the von Mises model with viscoplastic nonlinear isotropic hardening. It is noted that such problems feature in involving hardening material properties and weakening behavior corresponding to the strain-rate sensitivity in addition to widening deformation. Novelly, a unified mathematical and numerical treatment of plasticity and viscoplasticity problems is to be established. And the limiting cases of the current work are to be converted to the previous results [26,27].

2. Problem formulation

We start with the statement of a plane-strain viscoplasticity problem of the von Mises model with nonlinear isotropic hardening. Naturally, the problem statement leads to the lower bound formulation. The corresponding upper bound formulation can be stated by duality theorems [37,39,40,42] mainly following the work of Huh and Yang [16]. As shown by Yang [37,39,40,42], Huh and Yang [16], the duality theorem theoretically equates the greatest lower bound to the least upper bound. Therefore, we can approach the real limit solution by maximizing the lower bound or by minimizing the upper bound.

2.1. Problem statement (lower bound formulation)

We consider the general plane-strain problem with the domain D consisting of the static boundary ∂D_s and the kinematic boundary ∂D_k [40]. The quasi-static problem is to seek the maximum allowable driving load under constraints of static and constitutive admissibility such that

$$
\begin{aligned}
&\text{maximize} \quad q(\sigma) \\
&\text{subject to} \\
&\quad \nabla \cdot \sigma = 0 \quad \text{in } D, \\
&\quad \sigma \cdot \vec{n} = q\,\vec{t} \quad \text{on } \partial D_s, \\
&\quad \|\sigma\|_v \leqslant H(\bar{\varepsilon}, \dot{\bar{\varepsilon}}) \quad \text{in } D,
\end{aligned} \tag{1}
$$

where $\vec{n}$ indicates the unit outward normal vector of the boundary and the traction vector $\vec{t}$ is scalable distribution of the driving load on ∂D_s with the load factor q; $\|\sigma\|_v$ means the von Mises primal norm on stress tensor σ and the hardening function H is a function of the equivalent strain $\bar{\varepsilon}$ and the equivalent strain rate $\dot{\bar{\varepsilon}}$ describing viscoplastic strain-hardening. Therefore, this constrained problem is to sequentially maximize the load factor q representing the magnitude of the driving load for each step.

The primal problem (1) is the lower bound formulation seeking the extreme solution under constraints of static and constitutive admissibility. The statically admissible solutions satisfy the equilibrium equation and the static boundary condition. And the constitutive admissibility is stated by the yield criterion in an inequality form. We now refer to the work of Huh and Yang [16], Yang [42] to interpret the solutions as sets. First, the equilibrium equation is

linear and the constitutive inequality is convex and bounded. Accordingly, the intersection of statically admissible set and constitutively admissible set is convex and bounded. Moreover, the existence of a unique maximum to the convex programming problem is confirmed.

In the paper, the behavior of viscoplastic, nonlinear isotropic hardening is as adopted by Haghi and Anand [14]

$$
\begin{aligned}
H &= [\sigma_\infty - (\sigma_\infty - \sigma_0)\exp(-h\bar{\varepsilon})]\left(\frac{\dot{\bar{\varepsilon}}}{\dot{\bar{\varepsilon}}_0}\right)^m \\
&= \sigma_Y(\sigma_0, \sigma_\infty, \bar{\varepsilon})\left(\frac{\dot{\bar{\varepsilon}}}{\dot{\bar{\varepsilon}}_0}\right)^m,
\end{aligned}
\tag{2}
$$

where σ_0 is the initial yield strength, σ_∞ is the saturation stress and h is the hardening exponent. $\dot{\bar{\varepsilon}}_0$ and m are positive valued material parameters called the reference strain rate and strain rate sensitivity, respectively.

2.2. Upper bound formulation

Now we transform the lower bound formulation (1) to the upper bound formulation by restating equilibrium equations in a weak form as [23,26]

$$
\int_D \int_0^{\dot{\varepsilon}} \sigma : d\dot{\varepsilon}\, dA = q\left(\int_{\partial D_s} \vec{u}\cdot\vec{t}\, dS\right),
\tag{3}
$$

where $\vec{u}$ is a kinematically admissible velocity field. Further, according to the fundamental inequality for the mathematical plasticity or alternatively based on the concept of norms as stated in a generalized Hölder inequality by Yang [41], it results in

$$
\sigma : \dot{\varepsilon} = |\sigma : \dot{\varepsilon}| \leqslant \|\sigma\|_v \|\dot{\varepsilon}\|_{-v} = \bar{\sigma}\dot{\bar{\varepsilon}},
\tag{4}
$$

where $\|\dot{\varepsilon}\|_{-v}$ is the dual norm [16], on strain rate tensor $\dot{\varepsilon}$, of the von Mises primal norm $\|\sigma\|_v$ based on the associated flow rule. Note that equality holds if the normality condition in plasticity [12] is satisfied.

Thus, Eq. (3) can be then expressed as

$$
\begin{aligned}
q\left(\int_{\partial D_s} \vec{u}\cdot\vec{t}\, dS\right) &= \int_D \int_0^{\dot{\varepsilon}} \sigma : d\dot{\varepsilon}\, dA \\
&\leqslant \frac{\sigma_Y(\sigma_0, \sigma_\infty, \bar{\varepsilon})}{(1+m)\dot{\bar{\varepsilon}}_0^m}\int_D \|\dot{\varepsilon}\|_{-v}^{1+m}\, dA.
\end{aligned}
\tag{5}
$$

Note that, the velocity field $\vec{u}$ along the boundary ∂D_s is prescribed, e.g. $\vec{u}_s$, in each step. Therefore, we have

$$
\int_{\partial D_s} \vec{u}\cdot\vec{t}\, dS = G(\vec{u}_s, S),
\tag{6}
$$

where $G(\vec{u}_s, S)$ is a constant in each step but may be of various values in a process. Therefore, $q(\sigma)$ can be bounded above by $\bar{q}(\vec{u})$ as

$$
q(\sigma) \leqslant \frac{\sigma_Y(\sigma_0, \sigma_\infty, \bar{\varepsilon})}{(1+m)G\dot{\bar{\varepsilon}}_0^m}\int_D \|\dot{\varepsilon}\|_{-v}^{1+m}\, dA = \bar{q}(\vec{u}).
\tag{7}
$$

Therefore, the upper bound formulation is stated in the form of a constrained minimization problem as

$$
\begin{aligned}
&\text{minimize} \quad \bar{q}(\vec{u}) \\
&\text{subject to} \quad \bar{q}(\vec{u}) = \frac{\sigma_Y(\sigma_0, \sigma_\infty, \bar{\varepsilon})}{(1+m)G\dot{\bar{\varepsilon}}_0^m}\int_D \|\dot{\varepsilon}\|_{-v}^{1+m}\, dA, \\
&\qquad\qquad \nabla\cdot\vec{u} = 0 \quad \text{in } D, \\
&\qquad\qquad \text{kinematic boundary conditions on } \partial D_k,
\end{aligned}
\tag{8}
$$

where $\nabla\cdot\vec{u} = 0$ is the incompressibility constraint inherent in the von Mises-type materials. Therefore, the upper bound formulation seeks sequentially the least upper bound for each step on kinematically admissible solutions. Further, it is a basic assumption as adopted by Le Tallec [24] that the dissipation potential is a convex function in viscoplasticity. Accordingly, the primal–dual problems (1) and (8) are convex programming problems following the work of Huh and Yang [16] and Yang [42]. Thus, for each step, there exist a unique maximum and minimum to problems (1) and (8), respectively. Therefore, the extreme values of the lower bound functional $q(\sigma)$ and its corresponding upper bound functional $\bar{q}(\vec{u})$ are equal to the unique, exact solution q^* for each step in a process.

3. Computations

Traditionally, it is critical to make suitable assumptions of failure mechanisms corresponding to statically admissible stress field or kinematically admissible velocity field [6] to reduce the duality gap between the lower bound and the upper bound. However, by the use of finite element methods [33] together with mathematical programming techniques [25], limit analysis can be applied effectively to more complex problems.

3.1. Discretized functional

The upper bound formulation turns out to a constrained quadratic programming problem. The constrained minimization problem (8) is then stated approximately in the finite-element discretized form such that

$$
\begin{aligned}
&\text{minimize} \quad \tilde{q}(\{U\}) = \sum_{e=1}^{N_e} \frac{\sigma_Y(\sigma_0, \sigma_\infty, \bar{\varepsilon})}{1+m}\left(\sqrt{\{U\}^t[K_e]\{U\}}\right)^{1+m} \\
&\text{subject to} \quad \{U\}^t\{C\} = 0,
\end{aligned}
\tag{9}
$$

where N_e denotes the numbers of elements used to discretize the domain; $\{U\}$ is the nodal-point velocity vector and superscript t denotes transposition; $[K_e]$ is the element stiffness matrix combining with $G\dot{\bar{\varepsilon}}_0^m$, $\{C\}$ is a coefficient matrix.

3.2. Numerical algorithm

The CSSA algorithm presented by Yang [38] is now extended to deal with the nonlinear problem (9) sequentially. Accordingly, the functional at the current step n is reorganized in the following form:

minimize $\quad \breve{q}(\{U\}) = \sum_{e=1}^{N_e} \sigma_Y(\sigma_0, \sigma_\infty, \bar{\varepsilon}^n) \dfrac{\{U\}_{j+1}^t [K_e] \{U\}_{j+1}}{(\{U^*\}_j^t [K_e] \{U^*\}_j)^{(1-m)/2}}$

subject to $\ \{U\}_{j+1}^t \{C\} = 0,$

$$(10)$$

where subscripts j, $(j+1)$ on variables indicate that variables are corresponding to any successive iterations in each step. Note that the denominator in Eq. (10) is smoothed by a small real number δ to overcome the numerical difficulty corresponding to non-smoothness over some rigid regions as detailed by Huh and Yang [16], Leu and Chen [28]. At the first step, we have the equivalent strain $\bar{\varepsilon}^1 = 0$. For the current step $n \geqslant 2$, the value of $\bar{\varepsilon}^n$ is obtained as the following expression:

$$\bar{\varepsilon}^n = \sum_{i=1}^{n-1} \dot{\varepsilon}_i \Delta t_i, \tag{11}$$

where Δt_i is the step size.

In the computations, the penalty function method [32] is applied to establish the corresponding unconstrained functional. In problem (10), $\{U\}_{j+1}$ is the unknown at the current iteration $(j+1)$ with $\{U^*\}_j$ calculated at the preceding iteration j. For the case $j = 0$, an arbitrary $\{U\}_0$ is adopted to start the iterations. A monotonically convergent sequence of $\tilde{q}(\{U^*\}_j)$ is then generated iteratively. Based on the ratio of Euclidean norms, the convergence tolerance $E_U = \|\{U^*\}_j - \{U^*\}_{j-1}\|_2 / \|\{U^*\}_{j-1}\|_2$ is applied to check the convergence.

4. Convergence analysis

Before presenting numerical examples, we attempt to confirm the convergence of the extended general algorithm. First, we recall the Hölder inequality [13] in the following form:

$$\sum_{i=1}^n |x_i y_i| \leqslant \left[\sum_{i=1}^n |x_i|^p \right]^{1/p} \left[\sum_{i=1}^n |y_i|^q \right]^{1/q}, \tag{12}$$

where p, q are constants and $p > 1$ such that $1/p + 1/q = 1$ for any complex numbers $x_1, x_2, \ldots, x_n$; $y_1, y_2, \ldots, y_n$. Note that, the familiar Cauchy–Schwarz inequality [13] is the special case of the Hölder inequality [13] with $p = q = 2$.

Consider the following properties that:

$$\sigma_Y(\sigma_0, \sigma_\infty, \bar{\varepsilon}^n)(\{U^*\}_{j+1}^t [K_e] \{U^*\}_{j+1})^{(1+m)/2} \geqslant 0, \tag{13}$$

$$\sigma_Y(\sigma_0, \sigma_\infty, \bar{\varepsilon}^n) \frac{\{U^*\}_{j+1}^t [K_e] \{U^*\}_{j+1}}{(\{U^*\}_j^t [K_e] \{U^*\}_j)^{(1-m)/2}} \geqslant 0, \tag{14}$$

$$\sigma_Y(\sigma_0, \sigma_\infty, \bar{\varepsilon}^n)(\{U^*\}_j^t [K_e] \{U^*\}_j)^{(1+m)/2} \geqslant 0. \tag{15}$$

Thus, the Hölder inequality [13] can be applied to relate the discretized functional and its linearized expression in the following form:

$$\sum_{e=1}^{N_e} \sigma_Y(\sigma_0, \sigma_\infty, \bar{\varepsilon}^n)(\{U^*\}_{j+1}^t [K_e] \{U^*\}_{j+1})^{(1+m)/2}$$
$$\leqslant \left\{ \sum_{e=1}^{N_e} \sigma_Y(\sigma_0, \sigma_\infty, \bar{\varepsilon}^n) \frac{\{U^*\}_{j+1}^t [K_e] \{U^*\}_{j+1}}{(\{U^*\}_j^t [K_e] \{U^*\}_j)^{(1-m)/2}} \right\}^{(1+m)/2}$$
$$\cdot \left\{ \sum_{e=1}^{N_e} \sigma_Y(\sigma_0, \sigma_\infty, \bar{\varepsilon}^n)(\{U^*\}_j^t [K_e] \{U^*\}_j)^{(1+m)/2} \right\}^{(1-m)/2}. \tag{16}$$

Relating the inequalities (12) and (16), we have

$$1/p = (1+m)/2, \quad 1/q = (1-m)/2, \quad -1 < m < 1. \tag{17}$$

It is noted that $m = 0$ is corresponding to $p = q = 2$. Further, we can state the relation between the discretized functional and its linearized form as follows:

$$\sum_{e=1}^{N_e} \sigma_Y(\sigma_0, \sigma_\infty, \bar{\varepsilon}^n) \frac{\{U^*\}_{j+1}^t [K_e] \{U^*\}_{j+1}}{(\{U^*\}_j^t [K_e] \{U^*\}_j)^{(1-m)/2}}$$
$$\leqslant \sum_{e=1}^{N_e} \sigma_Y(\sigma_0, \sigma_\infty, \bar{\varepsilon}^n) \frac{\{U^*\}_j^t [K_e] \{U^*\}_j}{(\{U^*\}_j^t [K_e] \{U^*\}_j)^{(1-m)/2}}$$
$$= \sum_{e=1}^{N_e} \sigma_Y(\sigma_0, \sigma_\infty, \bar{\varepsilon}^n)(\{U^*\}_j^t [K_e] \{U^*\}_j)^{(1+m)/2}$$
$$= (1+m)\tilde{q}(\{U^*\}_j). \tag{18}$$

Therefore,

$$\sum_{e=1}^{N_e} \sigma_Y(\sigma_0, \sigma_\infty, \bar{\varepsilon}^n) \frac{\{U^*\}_{j+1}^t [K_e] \{U^*\}_{j+1}}{(\{U^*\}_j^t [K_e] \{U^*\}_j)^{(1-m)/2}}$$
$$\leqslant (1+m)\tilde{q}(\{U^*\}_j). \tag{19}$$

Combining the above-mentioned inequalities and recalling the following inequality proved by Goffman and Pedrick [13]:

$$A^{1/p} B^{1/q} \leqslant \frac{A}{p} + \frac{B}{q}, \quad A \geqslant 0, \ B \geqslant 0. \tag{20}$$

Accordingly, we obtain

$$(1+m)\tilde{q}(\{U^*\}_{j+1})$$
$$= \sum_{e=1}^{N_e} \sigma_Y(\sigma_0, \sigma_\infty, \bar{\varepsilon}^n)(\{U^*\}_{j+1}^t [K_e] \{U^*\}_{j+1})^{(1+m)/2}$$
$$\leqslant \left\{ \sum_{e=1}^{N_e} \sigma_Y(\sigma_0, \sigma_\infty, \bar{\varepsilon}^n) \frac{\{U^*\}_{j+1}^t [K_e] \{U^*\}_{j+1}}{(\{U^*\}_j^t [K_e] \{U^*\}_j)^{(1-m)/2}} \right\}^{(1+m)/2}$$
$$\cdot \left\{ \sum_{e=1}^{N_e} \sigma_Y(\sigma_0, \sigma_\infty, \bar{\varepsilon}^n)(\{U^*\}_j^t [K_e] \{U^*\}_j)^{(1+m)/2} \right\}^{(1-m)/2}$$
$$\leqslant \frac{1+m}{2}(1+m)\tilde{q}(\{U^*\}_j) + \frac{1-m}{2}(1+m)\tilde{q}(\{U^*\}_j)$$
$$= (1+m)\tilde{q}(\{U^*\}_j). \tag{21}$$

Thus, a series of monotonically convergent $\tilde{q}(\{U^*\}_j)$ are acquired such that

$$\tilde{q}(\{U^*\}_{j+1}) \leqslant \tilde{q}(\{U^*\}_j). \tag{22}$$

Therefore, the proof is completed with

$$\lim_{j \to \infty} \tilde{q}(\{U^*\}_j) = \tilde{q}^*, \tag{23}$$

where $\tilde{q}^*$ is the solution of the upper bound formulation (9) and the approximate value of the exact limit load factor q^*.

Consequently, the unconditional convergence of the CSSA algorithm has been proved by means of the Hölder inequality [13]. Moreover, the strain-rate sensitivity $m = 0$ is arithmetically equivalent to the indexes of the Hölder inequality $p = q = 2$ as shown in Eq. (17). On the other hand, the Cauchy–Schwarz inequality is a reduced form of the Hölder inequality with $p = q = 2$. Also, viscoplastic-ity problems are converted to rate independent plasticity problems if the strain-rate sensitivity $m = 0$ as seen in Eq. (2). Specifically speaking, it is then the familiar Cauchy–Schwarz inequality involved with convergence analysis of the CSSA algorithm while applied to rate independent plasticity problems. Note that Zhang et al. [43] conducted convergence analysis for a similar form of the CSSA algorithm specifically for rigid perfect plasticity problems. Accordingly, it can be deemed as a case study of the generalized framework shown in the paper with $m = 0$ and $p = q = 2$.

5. Analytical solutions

As detailed in the Appendix A.1, analytical solutions corresponding to thick-walled cylinders of strain-hardening viscoplastic materials subjected to internal pressure in plane-strain conditions was derived for rigorous comparisons. Note that the hardening exponent $h = \sqrt{3}$ is used in the derivations. With the boundary condition $\sigma_r(r = b) = 0$, we obtain the limit internal pressure in the form as

$$\frac{P_i}{\sigma_0} = \left(\frac{1}{\sqrt{3}}\right)^{m+1} \left(\frac{2V}{\dot{\bar{\varepsilon}}_0}\right)^m \left[\frac{1}{m}\left(\frac{a^m}{b^{2m}} - \frac{1}{a^m}\right)\right.$$
$$\left. + \frac{1}{m+1}\left(\frac{\sigma_\infty}{\sigma_0} - 1\right)(a_0^2 - a^2)\left(\frac{1}{a^{m+2}} - \frac{a^m}{b^{2m+2}}\right)\right], \tag{24}$$

where the innermost edge expanding uniformly at a constant speed V is used to simulate the action of internal pressure.

For the case with $m = 0$

$$\lim_{m \to 0} \frac{a^m b^{-2m} - a^{-m}}{m} = \ln\left(\frac{a^2}{b^2}\right). \tag{25}$$

Thus,

$$\frac{P_i}{\sigma_0} = \frac{1}{\sqrt{3}} \ln\left(\frac{a^2}{b^2}\right) + \frac{(\sigma_\infty/\sigma_0 - 1)}{\sqrt{3}}\left(\frac{a_0^2}{a^2} - \frac{b_0^2}{b^2}\right). \tag{26}$$

Note that, the sign convention for P_i is positive for tension and negative for compression. It is noted that analytical solutions for the first-step limit values are available in the literature for rigid perfect plasticity problems as presented by Jiang [21], Prager and Hodge [31].

For the case with $\sigma_\infty = \sigma_0$

$$\frac{P_i}{\sigma_0} = \frac{1}{m}\left(\frac{1}{\sqrt{3}}\right)^{m+1}\left(\frac{2V}{\dot{\bar{\varepsilon}}_0 a}\right)^m\left(\frac{a^{2m}}{b^{2m}} - 1\right). \tag{27}$$

It is also noted that analytical solutions for nonhardening viscoplasticity problems are available with the concept for the first-step limit values in the literature as presented by Peirce et al. [30].

6. Comparisons and validations

Comparisons between numerical results and analytical solutions are made as to show the reliable applications. We consider thick-walled cylinders made of strain-hardening viscoplastic materials subjected to internal pressure in plane-strain conditions. Especially, the present paper considers the viscoplastic, nonlinear isotropic strain-hardening behavior as shown in Eq. (2).

In the computations, the initial inner and outer radii are denoted as a_0 and b_0 respectively. The action of internal pressure is simulated with the innermost edge expanding uniformly at a constant speed V. The pressure needed to keep the expanding cylinder fully plastic is then computed sequentially by using the CSSA algorithm. In the following case studies, we adopt the consistently non-dimensional parameters: $a_0 = 5.0$, $b_0 = 10.0$, $h = \sqrt{3}$, $\dot{\bar{\varepsilon}}_0 = 1.0$, $V = 1.0$ and a constant step size $\Delta t = 0.001$.

As shown in Fig. 1, only one quarter of the axisymmetric structure is simulated. Four-node quadrilateral isoparametric elements are utilized to discretize the problem domain. Based on the mesh convergence study performed previously by Leu [26], the finite element mesh of 15×25 elements as shown in Fig. 1 is adopted in the following computations. Note that the first-step solution is the limit
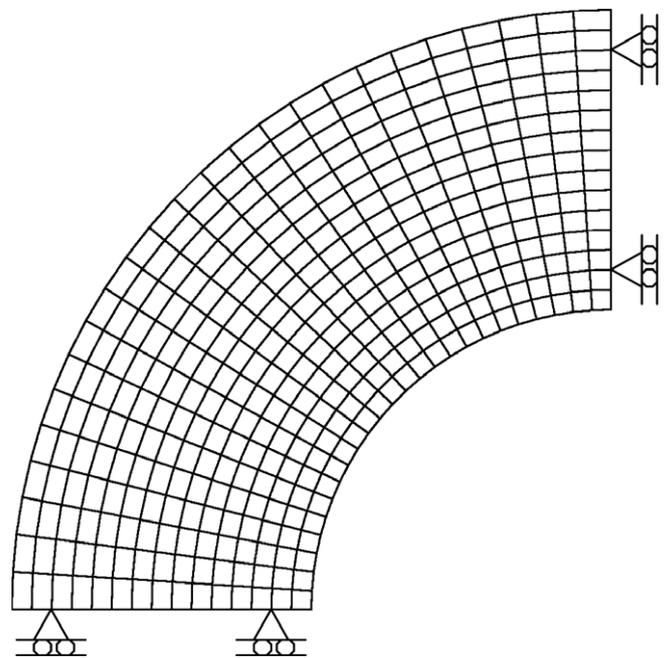

Fig. 1. Finite-element model of a thick-walled cylinder.

value of internal pressure causing the cylinder of dimensions a_0 and b_0 fully plastic. Following the first step, each step in sequential limit analysis starts with the result obtained in the preceding step and converges with one iteration for the specific problems concerned using the constant step size $\Delta t = 0.001$. A sequence of limit analysis problems is then solved to obtain sequential numerical solutions of deforming problems.

For the limiting case with $m = 0$, the problem is then converted to a rate independent plasticity problem involving strain-hardening materials. For the case with $\sigma_\infty = \sigma_0$, the problem is then reduced to a perfectly plasticity problem involving viscoplastic materials. Numerical cases are considered with various values of m and $R = \sigma_\infty / \sigma_0$. For each case, the cylinder is expanded to two times its initial inside radius. With an arbitrarily initial value $\{U\}_0$, the convergence tolerance $E_U = 0.001$ and the finite-element model shown in Fig. 1, the CSSA algorithm is accurate and efficient. The results, normalized by σ_0, of case studies under internal pressure are summarized in Fig. 2 for various hardening parameters ($R = \sigma_\infty / \sigma_0$) and strain-rate sensitivity $m = 0.1$. All the computed upper bounds agree very well with the analytical solutions at a modest cost.

The paper applies sequential limit analysis to deal with the widening problems featuring in hardening material properties and weakening behavior. The weakening behavior is corresponding to the strain-rate sensitivity m and widening deformation. As detailed in Appendix A.2, there exists strengthening phenomenon for $\sigma_\infty / \sigma_0 > 2$ if deforming cylinders are made of the strain-hardening materials with $h = \sqrt{3}$ and for the limiting case with $m = 0$. Therefore, there is no strengthening phenomenon for the case of $R = \sigma_\infty / \sigma_0 = 2$ with any strain-rate sensitivity m as illustrated in Fig. 3. Namely, the hollow cylinders of $\sigma_\infty / \sigma_0 > 2$ are strengthened until the onset of instability if the strain-hardening described by the Voce hardening law with
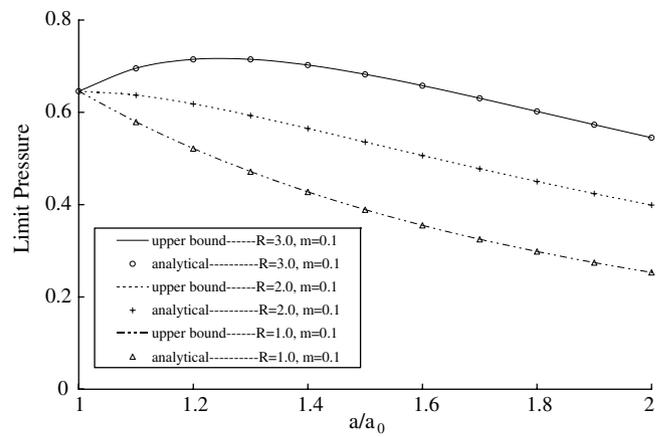

Fig. 2. Limit internal pressure versus inner radius with various hardening parameters ($R = \sigma_\infty / \sigma_0$) and strain-rate sensitivity $m = 0.1$.

$h = \sqrt{3}$ and for the limiting case with $m = 0$. Following that, however, the weakening phenomenon is observed due to the effect of the strain-hardening is counteracted by that of the strain-rate sensitivity m together with widening deformation. As shown in Fig. 4, there is strengthening phenomenon for the case of $R = \sigma_\infty / \sigma_0 = 2.2$ with $m = 0.0$, $m = 0.001$, $m = 0.3$. But there is no strengthening phenomenon for the cases of $m = 0.5$ and $m = 0.7$, respectively. However, the strengthening effect is dominant for the case of $R = \sigma_\infty / \sigma_0 = 2.5$. There is still strengthening phenomenon for the case of $R = \sigma_\infty / \sigma_0 = 2.5$ even for the case of $m = 0.7$ as shown in Fig. 5.

Note that, the onset of instability concerned above is about the plastic instability marked by the internal pressure maximum while dealing with thick-walled cylinders, see Leu and Chen [28]. Namely, the strengthening due to material hardening is exceeded by the weakening resulting from the strain-rate sensitivity m and widening deformation. As
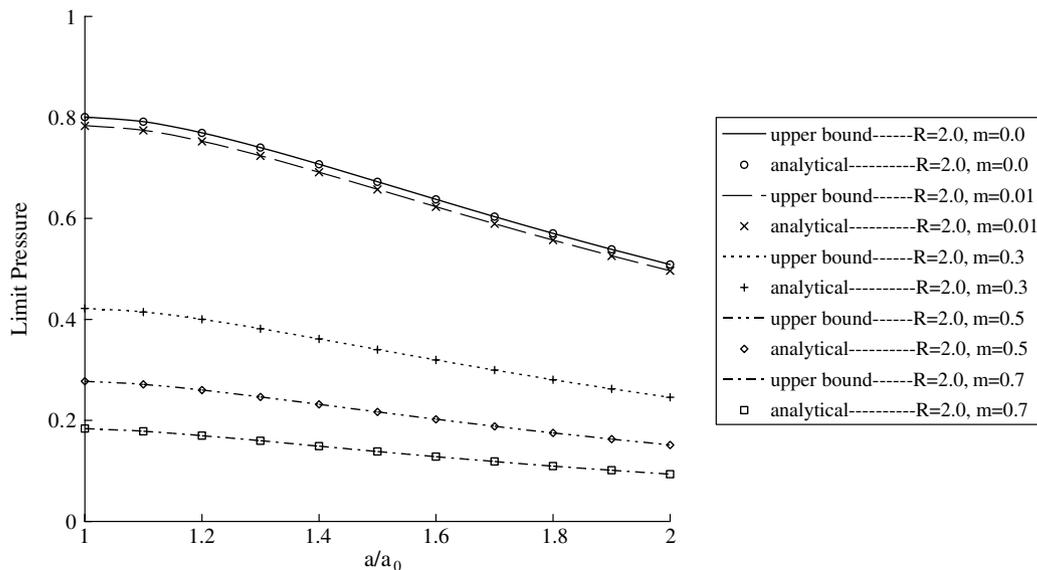

Fig. 3. Effect of strain-rate sensitivity m on limit internal pressure with $R = \sigma_\infty / \sigma_0 = 2.0$.
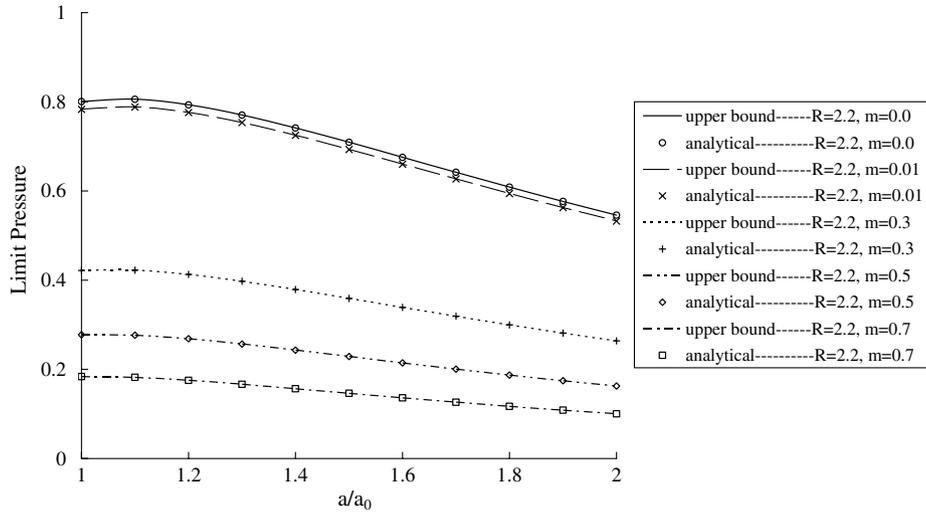
Fig. 4. Effect of strain-rate sensitivity m on limit internal pressure with $R = \sigma_\infty/\sigma_0 = 2.2$.
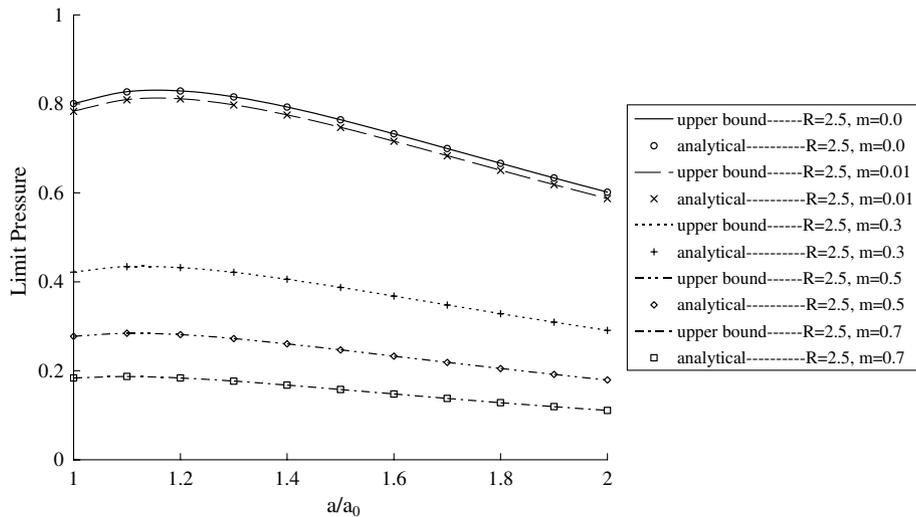

Fig. 5. Effect of strain-rate sensitivity m on limit internal pressure with $R = \sigma_\infty/\sigma_0 = 2.5$.

detailed in Appendix A.2, the onset of instability can be calculated by the following mathematical condition:

$$\frac{\partial(P_i/\sigma_0)}{\partial a} = 0. \tag{28}$$

Thus, corresponding to the initial inner and outer radii a_0, b_0, the strain-hardening described by the Voce hardening law with $h = \sqrt{3}$ and for the limiting case with $m = 0$, the onset of instability can be shown as

$$\frac{a}{a_0} = \sqrt{\frac{(b_0/a_0)^2 - 1}{X - 1}} \tag{29}$$

with the change of variables as follows:

$$X = \frac{\overline{A} + \sqrt{\overline{A}^2 + 4(b_0/a_0)^2}}{2}, \tag{30}$$

$$\overline{A} = \frac{(b_0/a_0)^2 - 1}{(\sigma_\infty/\sigma_0 - 1)}. \tag{31}$$

Note that, the stability condition for the widening problem of hollow cylinders depends on hardening material properties $R = \sigma_\infty/\sigma_0$, h and the strain-rate sensitivity m as shown in Figs. 3–5.

7. Conclusions

The paper had analytically and numerically studied thick-walled cylinders under internal pressure made of the von Mises materials with viscoplastic, nonlinear

isotropic hardening. Based on the concept of sequential limit analysis, problems were formulated as a sequence of limit analysis problems and solved iteratively by a combined smoothing and successively approximation (CSSA) algorithm. The CSSA algorithm adopted is comparable for its simple implementation and unconditional convergence. Especially, the Hölder inequality [13] was utilized to show the unconditional convergence of the CSSA algorithm. Analytical solutions were also derived in the paper for rigorous comparisons.

While performing the convergence analysis, it revealed an interesting implication relating the relationship of strain-rate sensitivity m and the indexes of the Hölder inequality p, q. The strain-rate sensitivity $m = 0$ is arithmetically equivalent to the indexes of the Hölder inequality $p = q = 2$. Moreover, the Cauchy–Schwarz inequality is a reduced form of the Hölder inequality with $p = q = 2$. Specifically speaking, it is then the familiar Cauchy–Schwarz inequality involved with convergence analysis of the CSSA algorithm while applied to rate independent plasticity problems ($m = 0$). In other cases, it is the Hölder inequality [13] showing the unconditional convergence of the CSSA algorithm.

Numerical and analytical studies in plane-strain deforming problems have demonstrated the accuracy of the numerical procedure presented here. The computed upper-bound results are in good agreement with analytical solutions at a modest cost. Attention was also paid to the strengthening phenomenon involving hardening material properties and weakening behavior resulting from the strain-rate sensitivity together with widening deformation.

Appendix A

A.1. Analytical solutions

It is supposed that the cylinder has its initial interior and exterior radii denoted by a_0 and b_0. It is clear that we consider a problem of widening deformation with the internal pressure being the driving load. As adopted by Haghi and Anand [14], the behavior of viscoplastic, nonlinear isotropic hardening is described by

$$\sigma_Y = [\sigma_\infty - (\sigma_\infty - \sigma_0) \exp(-h\bar{\varepsilon})] \left(\frac{\dot{\bar{\varepsilon}}}{\dot{\bar{\varepsilon}}_0} \right)^m, \tag{A.1}$$

where σ_0 is the initial yield strength, σ_∞ is the saturation stress and h is the hardening exponent. $\dot{\bar{\varepsilon}}_0$ and m are positive valued material parameters called the reference strain rate and strain rate sensitivity, respectively. For such deforming problems under external pressure, analytical solutions are available in the literature as presented by Haghi and Anand [14]. Analytical solutions for internal pressure are then derived in the following procedures similar to those adopted by the previous work of Leu [26,27] involving viscoplastic flow and nonlinear isotropic hardening problems, respectively.

In the cylindrical coordinate system, the incompressibility condition requires that

$$\frac{\partial v}{\partial r} + \frac{v}{r} = 0, \tag{A.2}$$

where v is the radial velocity at a point (r, θ). Further, if we consider a velocity control problem with the innermost edge expanding uniformly at a constant speed V. Then we can rewrite the radial velocity as

$$v = \frac{Va}{r}. \tag{A.3}$$

Accordingly, we can express the strain rates as

$$\dot{\varepsilon}_r = \frac{\partial v}{\partial r} = -\frac{Va}{r^2}, \tag{A.4}$$

$$\dot{\varepsilon}_\theta = \frac{v}{r} = \frac{Va}{r^2}, \tag{A.5}$$

$$\dot{\varepsilon}_z = 0 \tag{A.6}$$

and from Eqs. (A.4)–(A.6) we obtain the equivalent strain rate

$$\dot{\bar{\varepsilon}} = \sqrt{\frac{2}{3} (\dot{\varepsilon}_r^2 + \dot{\varepsilon}_\theta^2 + \dot{\varepsilon}_z^2)}. \tag{A.7}$$

And the equivalent strain is obtained as $\bar{\varepsilon} = \int \dot{\bar{\varepsilon}} \, dt$.

The components of the stress deviator, s_r, s_θ, s_z, can be obtained by considering the flow rule and satisfying the yield condition. Thus, we obtain

$$s_r = -\frac{1}{\sqrt{3}} [\sigma_\infty - (\sigma_\infty - \sigma_0) \exp(-h\bar{\varepsilon})] \left(\frac{\dot{\bar{\varepsilon}}}{\dot{\bar{\varepsilon}}_0} \right)^m, \tag{A.8}$$

$$s_\theta = \frac{1}{\sqrt{3}} [\sigma_\infty - (\sigma_\infty - \sigma_0) \exp(-h\bar{\varepsilon})] \left(\frac{\dot{\bar{\varepsilon}}}{\dot{\bar{\varepsilon}}_0} \right)^m, \tag{A.9}$$

$$s_z = 0. \tag{A.10}$$

Thus, the stresses are given as

$$\sigma_r = s + s_r, \tag{A.11}$$

$$\sigma_\theta = s + s_\theta, \tag{A.12}$$

$$\sigma_z = s + s_z, \tag{A.13}$$

where s is the mean normal stress.

Substituting Eqs. (A.11)–(A.13) into the following equilibrium equation:

$$\frac{\partial \sigma_r}{\partial r} + \frac{\sigma_r - \sigma_\theta}{r} = 0. \tag{A.14}$$

Therefore, we obtain

$$\frac{\partial \sigma_r}{\partial r} = \frac{2}{r} \left[\frac{\sigma_\infty}{\sqrt{3}} - \frac{\sigma_\infty - \sigma_0}{\sqrt{3}} \exp(-h\bar{\varepsilon}) \right] \left(\frac{\dot{\bar{\varepsilon}}}{\dot{\bar{\varepsilon}}_0} \right)^m. \tag{A.15}$$

Note that $h = \sqrt{3}$ is used in the derivations. With the boundary condition $\sigma_r(r = b) = 0$

$$\frac{P_i}{\sigma_0} = \left(\frac{1}{\sqrt{3}} \right)^{m+1} \left(\frac{2V}{\dot{\bar{\varepsilon}}_0} \right)^m \left[\frac{1}{m} \left(\frac{a^m}{b^{2m}} - \frac{1}{a^m} \right) \right.$$
$$\left. + \frac{1}{m+1} \left(\frac{\sigma_\infty}{\sigma_0} - 1 \right) (a_0^2 - a^2) \left(\frac{1}{a^{m+2}} - \frac{a^m}{b^{2m+2}} \right) \right]. \tag{A.16}$$

Note that, the sign convention for P_i is positive for tension and negative for compression.

For the case with $m = 0$

$$\lim_{m \to 0} \frac{a^m b^{-2m} - a^{-m}}{m} = \ln\left(\frac{a^2}{b^2}\right). \tag{A.17}$$

Thus, we reduce the viscoplasticity problems to rate independent plasticity problems with the strain rate sensitivity $m = 0$, such that

$$\frac{P_i}{\sigma_0} = \frac{1}{\sqrt{3}} \ln\left(\frac{a^2}{b^2}\right) + \frac{(\sigma_\infty/\sigma_0 - 1)}{\sqrt{3}} \left(\frac{a_0^2}{a^2} - \frac{b_0^2}{b^2}\right). \tag{A.18}$$

It is noted that analytical solutions for the first-step limit values of rigid perfect plasticity problems are available in the literature as presented by Jiang [21], Prager and Hodge [31].

For the case with $\sigma_\infty = \sigma_0$, we reduce to non-hardening power-law viscoplasticity problems such that

$$\frac{P_i}{\sigma_0} = \frac{1}{m}\left(\frac{1}{\sqrt{3}}\right)^{m+1} \left(\frac{2V}{\dot{\bar{\varepsilon}}_0 a}\right)^m \left(\frac{a^{2m}}{b^{2m}} - 1\right). \tag{A.19}$$

It is also noted that such analytical solution for non-hardening power-law viscoplasticity problems is available with the concept for the first-step limit values in the literature as presented by Peirce et al. [30].

A.2. Strengthening versus weakening

We come to consider the condition of stability, namely the existence of hardening phenomena before the weakening behavior. For simplicity, we consider the limiting cases with $m = 0$. To consider the existence of the maximum value of the limit pressure during the whole widening process, we apply the necessary condition for the maximum of P_i/σ_0, namely the following mathematical expression with the current interior radius a:

$$\frac{\partial(P_i/\sigma_0)}{\partial a} = 0. \tag{A.20}$$

It is noted that the following derivation is similar to that presented by Leu and Chen [28] dealing with plastic limit analysis of rotating hollow cylinders. Consider Eqs. (A.16) and (A.20), we get the stability condition in the form

$$\frac{b_0^2 - a_0^2}{\sigma_\infty/\sigma_0 - 1} = \frac{a_0^2}{a^2}(b_0^2 - a_0^2 + a^2) - \frac{a^2 b_0^2}{b_0^2 - a_0^2 + a^2}. \tag{A.21}$$

Further, we set

$$X = \frac{b_0^2 - a_0^2 + a^2}{a^2} = \frac{b^2 - a^2 + a^2}{a^2} = \frac{b^2}{a^2} > 1 \tag{A.22}$$

and

$$A = \frac{b_0^2 - a_0^2}{\sigma_\infty/\sigma_0 - 1} = a_0^2 \frac{(b_0/a_0)^2 - 1}{\sigma_\infty/\sigma_0 - 1} = a_0^2 \overline{A} \tag{A.23}$$

with

$$\overline{A} = \frac{(b_0/a_0)^2 - 1}{\sigma_\infty/\sigma_0 - 1}. \tag{A.24}$$

Thus, we can rewrite Eq. (A.21) as

$$X^2 - \overline{A}X - \frac{b_0^2}{a_0^2} = 0. \tag{A.25}$$

Accordingly, for given a_0/b_0 and σ_∞/σ_0, we can obtain the solution explicitly

$$X = \frac{\overline{A} + \sqrt{\overline{A}^2 + 4(b_0/a_0)^2}}{2}. \tag{A.26}$$

Then with the explicit expression of X, we can identify the onset of instability from Eq. (A.22) as

$$a/a_0 = \sqrt{\frac{(b_0/a_0)^2 - 1}{X - 1}}. \tag{A.27}$$

Finally, we come to consider the existence of hardening phenomena before the weakening behavior. Certainly, it is to see if Eq. (A.27) has the solution $a/a_0 > 1$. According to Eqs. (A.23), (A.26) and (A.27), we can get the stability condition for the limiting cases with $m = 0$ as

$$\sigma_\infty/\sigma_0 > 2. \tag{A.28}$$

Therefore, if deforming cylinders are made of the strain-hardening materials described by the Voce hardening law with $h = \sqrt{3}$, then for the limiting cases with $m = 0$ there exists strengthening phenomenon for $\sigma_\infty/\sigma_0 > 2$.

References

[1] E. Anderheggen, H. Knöpfel, Finite element limit analysis using linear programming, Int. J. Solids Struct. 8 (1972) 1413–1431.

[2] C. Bohatier, J.L. Chenot, Finite element formulations for non-steady-state large viscoplastic deformation, Int. J. Numer. Methods Engrg. 21 (1985) 1697–1708.

[3] A. Bottero, R. Negre, J. Pastor, S. Turgeman, Finite element method and limit analysis theory for soil mechanics problems, Comput. Methods Appl. Mech. Engrg. 22 (1980) 131–149.

[4] H.L. Cao, M. Potier-Ferry, An improved iterative method for large strain viscoplastic problems, Int. J. Numer. Methods Engrg. 44 (1999) 155–176.

[5] A. Capsoni, L. Corradi, A finite element formulation of the rigid-plastic limit analysis problem, Int. J. Numer. Methods Engrg. 40 (1997) 2063–2086.

[6] W.F. Chen, Limit Analysis and Soil Plasticity, Elsevier, Amsterdam, 1975.

[7] E. Christiansen, Computation of limit loads, Int. J. Numer. Methods Engrg. 17 (1981) 1547–1570.

[8] L. Corradi, N. Panzeri, C. Poggi, Post-critical behavior of moderately thick axisymmetric shells: a sequential limit analysis approach, Int. J. Struct. Stabil. Dynam. 1 (2001) 293–311.

[9] L. Corradi, N. Panzeri, A triangular finite element for sequential limit analysis of shells, Adv. Engng. Software 35 (2004) 633–643.

[10] L. Corradi, L. Luzzi, P. Vena, Finite element limit analysis of anisotropic structures, Comput. Methods Appl. Mech. Engrg. 195 (2006) 5422–5436.

[11] N. Dang Hung, Direct limit analysis via rigid-plastic finite elements, Comput. Methods Appl. Mech. Engrg. 8 (1976) 81–116.

[12] D.C. Drucker, A definition of stable inelastic material in the mechanics of continua, J. Appl. Mech. 81 (1959) 101–106.

[13] C. Goffman, G. Pedrick, First Course in Functional Analysis, Prentice-Hall, Englewood Cliffs, NJ, 1965.

[14] M. Haghi, L. Anand, Analysis of strain-hardening viscoplastic thick-walled sphere and cylinder under external pressure, Int. J. Plasticity 7 (1991) 123–140.

[15] P.G. Hodge, T. Belytschko, Numerical methods for the limit analysis of plates, J. Appl. Mech. 35 (1968) 796–802.

[16] H. Huh, W.H. Yang, A general algorithm for limit solutions of plane stress problems, Int. J. Solids Struct. 28 (1991) 727–738.

[17] H. Huh, C.H. Lee, Eulerian finite-element modeling of the extrusion process for working-hardening materials with the extended concept of limit analysis, J. Mater. Process. Technol. 38 (1993) 51–62.

[18] H. Huh, C.H. Lee, W.H. Yang, A general algorithm for plastic flow simulation by finite element limit analysis, Int. J. Solids Struct. 36 (1999) 1193–1207.

[19] C.L. Hwan, An upper bound finite element procedure for solving large plane strain deformation, Int. J. Numer. Methods Engrg. 40 (1997) 1909–1922.

[20] G.L. Jiang, Regularized method in limit analysis, J. Engrg. Mech. 120 (1994) 1179–1197.

[21] G.L. Jiang, Nonlinear finite element formulation of kinematic limit analysis, Int. J. Numer. Methods Engrg. 38 (1995) 2775–2807.

[22] K.P. Kim, H. Huh, Dynamic limit analysis formulation for impact simulation of structural members, Int. J. Solids Struct. 43 (2006) 6488–6501.

[23] S. Kobayashi, A review on the finite-element method and metal forming process modeling, J. Appl. Metalworking 2 (1982) 163–169.

[24] P. Le Tallec, Numerical solution of viscoplastic flow problems by augmented Lagrangians, IMA J. Numer. Anal. 6 (1986) 185–219.

[25] D.G. Luenberger, Linear and Nonlinear Programming, Addison-Wesley, MA, 1984.

[26] S.-Y. Leu, Limit analysis of viscoplastic flows using an extended general algorithm sequentially: convergence analysis and validation, Comput. Mech. 30 (2003) 421–427.

[27] S.-Y. Leu, Convergence analysis and validation of sequential limit analysis of plane-strain problems of the von Mises model with nonlinear isotropic hardening, Int. J. Numer. Methods Engrg. 64 (2005) 322–334.

[28] S.-Y. Leu, J.T. Chen, Sequential limit analysis of rotating hollow cylinders of nonlinear isotropic hardening, Comput. Model. Engrg. Sci. 14 (2006) 129–140.

[29] J. Pastor, T-H. Thai, P. Francescato, New bounds for the height limit of a vertical slope, Int. J. Numer. Anal. Methods Geomech. 24 (2000) 165–182.

[30] D. Peirce, C.F. Shih, A. Needleman, A tangent modulus method for rate dependent solids, Comput. Struct. 18 (1984) 875–887.

[31] W. Prager, P.G. Hodge, Theory of Perfectly Plastic Solids, John Wiley and Sons, New York, 1951, pp. 115–118.

[32] J.N. Reddy, Applied Functional Analysis and Variational Methods in Engineering, McGraw-Hill, New York, 1986.

[33] J.N. Reddy, An Introduction to the Finite Element Method, McGraw-Hill, New York, 1993.

[34] S.W. Sloan, Upper bound limit analysis using finite elements and linear programming, Int. J. Numer. Anal. Methods Geomech. 13 (1989) 263–282.

[35] Y. Tomita, R. Sowerby, An approximate analysis for studying the deformation mechanics of rate sensitive materials, Int. J. Mech. Sci. 20 (1978) 361–371.

[36] F. Voldoire, Regularized limit analysis and applications to the load carrying capacities of mechanical components, in: Proc. European Congress on Computational Methods in Applied Sciences and Engineering, Barcelona, 2000.

[37] W.H. Yang, Minimization approach to limit solutions of plates, Comput. Methods Appl. Mech. Engrg. 28 (1981) 265–274.

[38] W.H. Yang, A variational principle and an algorithm for limit analysis of beams and plates, Comput. Methods Appl. Mech. Engrg. 33 (1982) 575–582.

[39] W.H. Yang, A duality theorem for plastic plates, Acta Mech. 69 (1987) 177–193.

[40] W.H. Yang, Admissibility of discontinuous solutions in mathematical models of plasticity, in: W.H. Yang (Ed.), Topics in Plasticity, AM Press, MI, 1991.

[41] W.H. Yang, On generalized Hölder inequality, Nonlinear Anal.: Theory Methods Appl. 16 (1991) 489–498.

[42] W.H. Yang, Large deformation of structures by sequential limit analysis, Int. J. Solids Struct. 30 (1993) 1001–1013.

[43] Y.G. Zhang, P. Zhang, W.M. Xue, Limit analysis considering initial constant loadings and proportional loadings, Comput. Mech. 14 (1994) 229–234.